Oceanological and Hydrobiological Studies

International Journal of Oceanography and Hydrobiology

Volume 55, No. 1 March 2026
pages (73-90)

ISSN 1730-413X
eISSN 1897-3191

Day-to-day statistical and spatio-temporal analysis of cyclone Mocha (2023) induced cold wake and sea surface height anomalies through multi-resolution satellite data and cloud computing

by

Priyanka Puri*,[a]

DOI: **https://doi.org/10.26881/oahs-2026.1.06**
Category: **Original research papers**
Received: **November 28, 2025**
Accepted: **February 25, 2026**

Department of Geography, Miranda House, University of Delhi, Delhi-110007, India

[a] *(https://orcid.org/0000-0002-8232-998X)*

Abstract

As an intense tropical cyclone (TC) formed over the Bay of Bengal (BoB) in May 2023, Cyclone Mocha provides a significant opportunity to examine upper ocean responses to cyclonic forcing. Here, a spatio-temporal analysis has been done for cyclone induced Cold wake and sea surface height (SSH) changes through high-resolution daily satellite datasets combined with cloud computing through Google Earth Engine (GEE) and statistical analysis supported by Python-based processing. Buffering a spatial extent of 300 km along the cyclone track, the pre-cyclone period of 15 days was taken as the baseline for examination, 15th April'23–1st May'23, with a broader examination attempted from 15th April to 31st May' 2023. Results indicated a strong cold wake occurring along Mocha's track with sea surface temperature (SST) falling by around 2°C. Sea Surface Height Anomaly SSHA exhibited a moderate positive relationship with SST and a weaker recovery. The statistical interpretation from the results of Pearson's correlation, Linear Trends and Causality (Granger) indicated a specific impact of the cyclone on SST and SSHA. The results validated cyclone- ocean interactions with strong indications of spatial and temporal alignment of regional dynamics, wind, SST and SSH. It also highlighted the strength of cloud computing and satellite outputs for ocean monitoring, forecasting, re-analysis, and resilience.

Key words: cyclone, Mocha, Bay of Bengal, cold wake, anomalies

* Corresponding author: *priyanka.puri@mirandahouse.ac.in*

1. Introduction

Considered as the most destructive phenomena of tropical coastal meteorology, tropical cyclones (TCs) are outcomes of strong oceanic and atmospheric interface (Mittal et al., 2019; Murty et al., 1986; Oginni et al., 2021; Singh & Roxy, 2022; Srinivas et al., 2016; Subbaramayya and Rao, 1984). Their negative impacts are exhibited in the form of immense loss of life and property besides posing substantial risk to human life, property, marine ecosystems, and oceans (Das & Debnath, 2017; Dube et al., 2009; Karnauskas et al., 2021; Mukherjee et al., 2024; Ortiz et al., 2023; Pathirana & Priyadarshani, 2022; Sala et al., 2024).

TC genesis and intensification are intricately linked to the ocean's upper layer thermal structure (Cione & Uhlhorn, 2003; Emanuel, 1986; Kranthi et al., 2022; Price, 2009) and deep ocean heat content as they provide fuel (Balaguru et al., 2012; Shay et al., 2000) to this thermal engine (Makarieva et al., 2008). These operate impacting each other in the form of Tropical Cyclone Heat Potential and the Upper Ocean Heat Content (Akhila et al., 2025; Albert & Bhaskaran, 2020; Ali et al., 2011; Oey et al., 2007).

They also generate significant responses over the ocean surface observed in the form of thermocline shoaling, near-inertial currents, surface cooling, subsurface warming, and changes in salinity stratification, change in SSH, anomaly generation in SST and SSH, vertical mixing, upwelling and increase in SSH following the cyclone path (Akhila et al., 2022, 2025; Chacko & Jayaram, 2022; Cheng et al., 2013; Das et al., 2025; Gopalan et al., 2000; Jourdain et al., 2013; Karnauskas et al., 2021; Kuttippurath et al., 2022; Nelson, 1996; Oey et al., 2007; Price, 1981; Price et al., 1994; Ren et al., 2024; Roxy et al., 2014; Sala et al., 2024; Suda, 1943; Yu et al., 2023; Zhang et al., 2023; Zhao et al., 2022).

SSH and SSHA are key indicators of ocean dynamics during cyclones. In this category, cold wakes are a distinct phenomenon. They are large size in and wide in area (Pasquero et al., 2021) and can directly impact cyclone strength and further atmospheric feedback processes for the TCs (Goni & Trinanes, 2011; Lloyd & Vecchi, 2011; Zhao et al., 2022). They can be salty (Singh & Roxy, 2022) and can last for a minimum of one day to several days (Dare & Bride, 2011; Kerhalkar et al., 2025), weeks (Pasquero et al., 2021), and even a month (Karnauskas et al., 2021) with impacts on SST remaining even beyond a month (Karnauskas et al., 2021).

These are formed due to a cyclone's intense wind stress, which causes a redistribution of ocean water masses resulting in elevated or depressed SSH from the existing with anomalies associated with storm surge, coastal flooding, and upwelling-downwelling phenomena in the ocean due to wind stress, circulation of ocean waters and resultant pumping (D'Asaro et al., 2011; Navaneeth et al., 2019; Sanford et al., 2007; Vinayachandran et al., 2002). SSH and SSHA are other key indicators of ocean dynamics during cyclones as they enhance vertical mixing, which influences the distribution of heat, salt, and nutrients in the upper ocean (Busireddy et al., 2019; Maneesha et al., 2011; Ramachandran et al., 2018; Vinayachandran et al., 2002; Vinaychandran & Mathew, 2003).

Monitoring SSH variations helps to understand cyclone-ocean interactions and assess the potential for cyclone intensification or weakening (Bernier et al., 2024; Kuttippurath, 2022). Studies have shown that strong storms trigger SST cooling ranging from 1°C to 6°C, depending on pre-storm conditions, cyclone intensity, and translation speed (Karnauskas et al., 2021; Kuttippurath et al., 2022; Sadhuram, 2004; Schade & Emanuel, 1999; Yu et al., 2023). However, the identification of cold wakes in terms of their area or duration has no fixed criterion and is dependent on climatology undertaken as per study (John et al., 2025; Karnauskas et al., 2021; Kuttippurath et al., 2022). The Bay of Bengal (BoB) is highly prone to tropical cyclogenesis due to its warm surface, high ocean heat content, and suitable atmospheric conditions (Elizabeth et al., 2020; Kuttippurath, 2022; Selva et al., 2025; Shenoi et al., 2002; Singh & Roxy, 2022; Subbaramayya and Rao, 1984).

1.1. Study area

The BoB is the largest Bay in the world (Xia et al., 2023). The location of BoB can be seen in Fig. 1.

It is a vast and ecologically significant segment of the northern Indian Ocean, lying approximately between 5°N–22°N latitude and 80°E–100°E longitude. It stretches about 2090 km in length and 1610 km in width (Mohanty et al., 2008) and is flanked by the eastern coastline of India, the western shores of Myanmar, and bordered to the south by Bangladesh, Sri Lanka, and the Andaman and Nicobar Islands. A semi-enclosed basin, the BoB is unique (Shenoi et al., 2002), active (Prakash & Pant, 2020), and is known for its high frequency of severe cyclonic storms, especially during the pre-monsoon (April–June) and post-monsoon (October–December) periods; guided by geography, climate and complex ocean-atmosphere interactions (Alamgir et al., 2025; Busireddy et al., 2019; Elizabeth et al., 2020; Kodunthirapully Narayanaswami & Ramasamy, 2022; Kranthi et al., 2022; Kumar et al., 2024; Kuttippurath et al., 2022; Selva et al., 2025; Subbaramayya and Rao, 1984). May and November

Journal owner: Faculty of Oceanography and Geography, University of Gdańsk, Poland

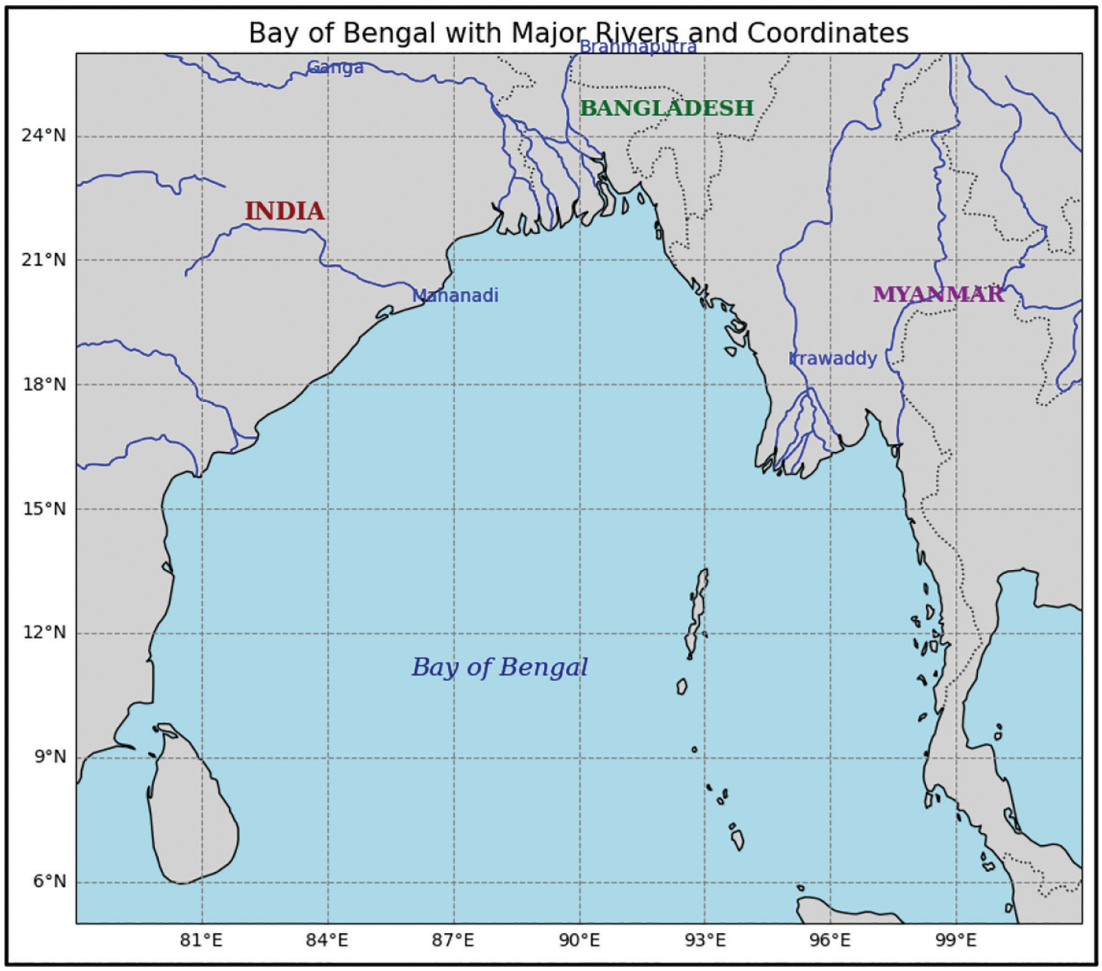

Figure 1

Study area - Location. *Source*: Author (2025).

are the peak months of TC formation (Alam et al., 2003; Albert & Bhaskaran, 2020).

It is particularly vulnerable due to its shallow bathymetry, warm SSTs, and dense coastal population (Webster et al., 2005). Cyclones over the BoB tend to intensify rapidly, drawing energy from the warm surface waters and interacting with mesoscale oceanic features such as eddies and salinity fronts (Ji et al., 2021; Singh & Roxy, 2022).

Sharp salinity and temperature gradients (Sengupta et al., 2006; Shetye et al., 1996; Vinayachandran et al., 2002) contribute to strong vertical stratification. This significantly influences cyclone-ocean feedback mechanisms, such as cold wake formation and ocean heat content variability (Roxy et al., 2014). Influx of vast quantities of fresh waters from the Ganga–Brahmaputra–Meghna (GBM) river system (Vinayachandran et al., 2002) tends to create a barrier layer associated salinity changes have a large role in play in the TC dynamics in the region (Alamgir et al., 2025; Kerhalkar et al., 2025; Kumar et al., 2024; Kuttippurath et al., 2022; Mohanty et al., 2008; Neetu et al., 2012; Prakash & Pant, 2020; Sengupta et al., 2006; Vissa et al., 2013; Yu et al., 2023).

This fresh water influx and the existence of a mixed layer of water has a pertinent role to play in TC dynamics in the BoB (Jarugula & McPhaden, 2022; Kumar et al., 2024). Warm and cold core mesoscale eddies have been recorded to significantly impact the TC dynamics in BoB where they are found in abundance (Akhila et al., 2025; Kodunthirapully Narayanaswami & Ramasamy, 2022; Walker et al., 2005). Recently, cold wakes have been documented in the BoB for Phailin (Kuttippurath et al., 2022) and Amphan cyclones (Akhila et al., 2025).

Shallow continental shelves enhance surge heights and reduce frictional energy loss because water cannot disperse vertically and is instead pushed landward, leading to severe flooding (Dube et al., 2009) and allowing cyclones to sustain intensity longer near coasts

(Murty et al., 1986). In the BoB, cold wake recovery is often slower due to strong salinity stratification from river runoff, which creates a shallow barrier layer (Vinayachandran et al., 2002), inhibits vertical mixing reversal and delays heat recharge (Kerhalkar et al., 2025). However, in specific cases, a wake might not even form (Jarugula & McPhaden, 2022).

1.2. Relevance and objectives of the study

Cyclone Mocha is recorded as the strongest cyclone on record for the North Indian Ocean (NASA Earth Observatory, 2023). Described as an 'extremely severe cyclonic storm' (World Bank, 2023), it originated as a low-pressure system in the central BoB as the first cyclone of the season (Sharma et al., 2024). Starting from 8th May, it made landfall on 14th May near the Myanmar-Bangladesh border, causing extensive damage and human displacement (World Bank, 2023). Within a few days (IMD, 2023), it reached a peak intensity with wind speeds of approximately 280 km · h^{-1} by 14 May 2023. It is also seen as one of the strongest cyclones in the BoB during the 21st century (IMD, 2023; JTWC, 2023; NASA Earth Observatory, 2023).

Mocha's rapid intensification as Category 5 storm has been linked to unusually warm ocean surface temperatures and the presence of subsurface heat reservoirs (Sharma et al., 2024), such as barrier layers and mixed layer eddies (Kerhalkar et al., 2025) and focusses specificity to be studied (Lin et al., 2009). However, Mocha still remains less explored in terms of a spatio-temporal study and more so in the context of cold-wake and SSH behaviour. Table 1 and Fig. 2 show the locational aspects of the cyclone.

The current work attempts to follow a baseline of about 15 days before the TC and 15 days post TC Mocha landfall to observe and analyze the phenomenon, ranging from 15th April'23 to 31st May'23. The baseline period is taken from 15th April'23 to 1st May' 23, with the cyclone period of 9th–15th May specifically the focus. The aims of the study are:

a. To identify if any cold wake existed via SST anomalies due to cyclone Mocha along its track, buffered at 300 km to get a specified overview.
b. To analyze the spatial and temporal evolution of SST, SSH, cold wake trend and anomalies due to Mocha along the buffered track.
c. To observe the interrelationship between SST and SSH trends and anomalies arising due to Mocha along the buffered track.

Table 1

Locational and meteorological details of cyclone Mocha'23.

Latitude	Longitude	Pressure_hPa	Wind_speed_knots
11.10	88.19	994	35
11.39	88.09	991	45
11.99	88.09	990	51
12.80	88.09	984	60
13.4	88.19	981	64
13.99	88.30	981	74
14.60	88.69	966	89
15.00	88.69	960	109
15.30	89.10	955	115
15.99	89.99	955	115
16.89	90.80	923	128
17.80	91.09	923	128
18.70	91.80	919	138
19.80	92.49	918	134
20.79	93.09	946	105
22.99	94.69	984	54
11.22	88.14	992	40
11.66	88.09	990	48
12.39	88.09	987	55
13.11	88.14	982	62
13.69	88.22	981	69
14.31	88.50	973	81
14.82	88.70	963	99
15.12	88.83	957	112
15.60	89.51	955	115
16.43	90.44	939	121
17.34	90.95	923	128
18.23	91.42	921	133
19.24	92.15	918	136
20.21	92.73	932	119
21.77	93.79	965	79

Source: Author, 2025 from 'NOAA/IBTrACS/v4' from GEE.
GEE, Google Earth Engine.

The study operates on multiple- resolution scales, cloud computing datasets derived from Google Earth Engine (GEE), which are processed further in Python. The significance of the content and methodology is that it tends to keep the focus on the outputs generated by cyclone Mocha rather than being basin-oriented to avoid anomalies. Spatial buffering of the track marks a relevant impact zone for the cyclone in the entirety of its occurrence in the BoB. This makes the results highly

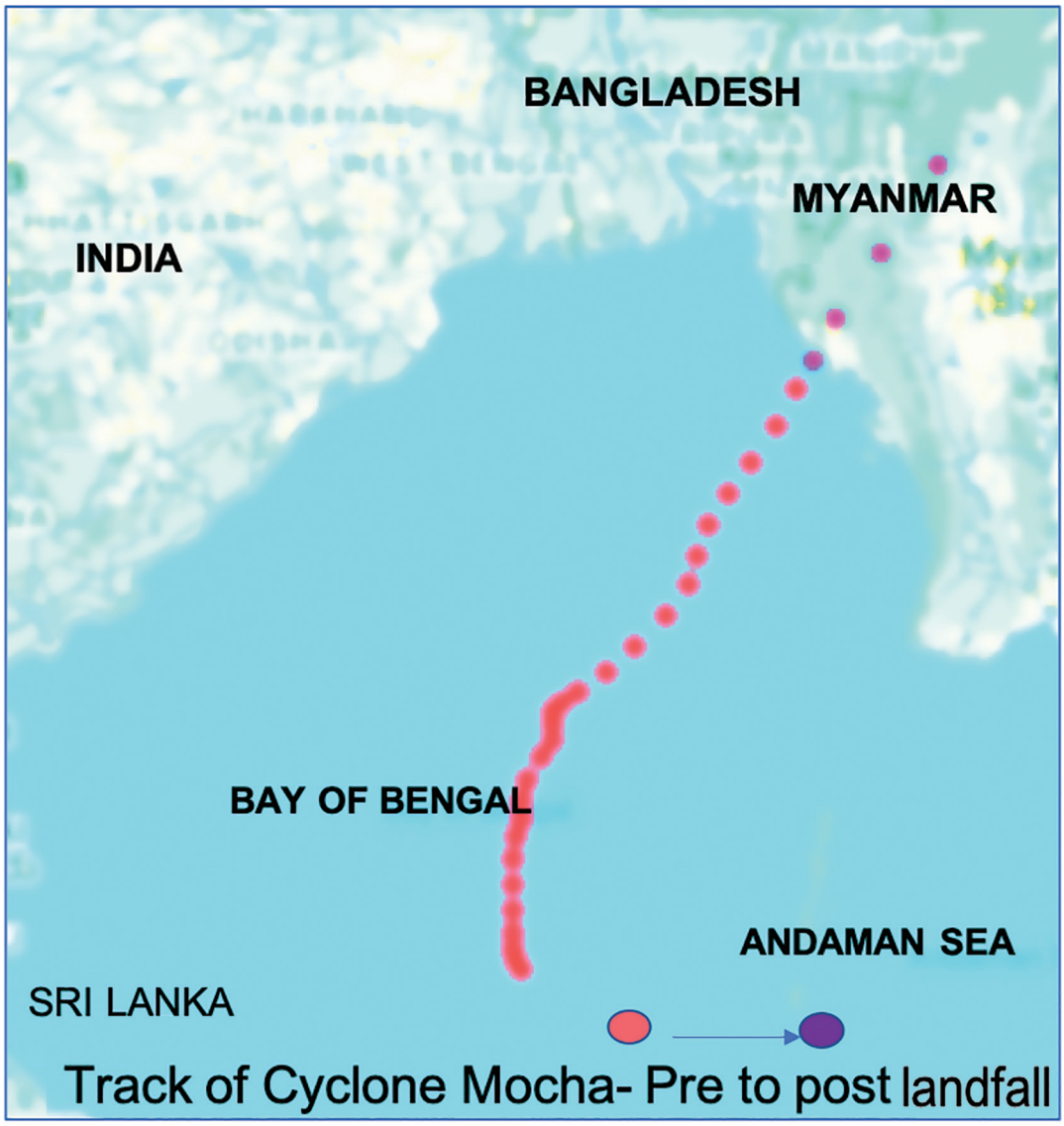

Figure 2

Track of cyclone Mocha (2023)—from pre- to post-landfall. (Track of cyclone Mocha from pre to post (pink color) to post-landfall (purple color). *Source*: Author, 2025 from 'NOAA/IBTrACS/v4' from GEE. GEE, Google Earth Engine.

correlated with the development and advancement of the cyclone rather than being subdued by processes outside its zone of influence in the basin. The error margin was greatly reduced through this method, over which a statistical interpretation has been applied. Spatial and temporal mapping has further facilitated interpretations of the parameters.

2. Materials and methods

This study investigates the spatio-temporal dynamics of cold wake and SSHA induced by Cyclone Mocha (2023) over the BoB on a day-to-day scale. The methodology begins from track identification of the cyclone from its latitudinal and longitudinal extent during its complete phase of development to landfall. This was followed by drawing a spatial buffer of 300 km along the track to have the output cyclone-specific rather than entire BoB oriented. This information was derived from GEE from the 'NOAA/IBTrACS/v4' database. 31 points from inception to pre-landfall and 4 points post-landfall were extracted and plotted. The International Best Track Archive for Climate Stewardship (IBTrACS) from National Oceanic and Atmospheric Administration (NOAA) National

Centers for Environmental Information (NCEI) is a database for deriving the location and intensity of TCs across the world. The data is given from 1842 to the present at a three-hourly interval. This basin-wise data is focused upon position and intensity of the cyclone derived from minimum central pressure or maximum sustained wind speed as parameters (Google Earth Engine, 2025).

The track co-ordinates derived from the NOAA NCEI database were subjected to a buffering of 300 km for SST derivation from the NOAA/CDR/OISST/V2_1 dataset via cloud computing through GEE. Considered as a medium resolution dataset at a scale of 27.8 km, it provided information on SST at ¼ degree via Optimum Interpolation SST. Cold wake area and other related information are drawn from the same. Data availability from 1981 onwards is derived from satellites, buoys, and ships and is processed twice daily. The gaps are filled with interpolation, and the advanced very high resolution radiometer (AVHRR) enables it to provide a high spatio-temporal coverage (NOAA, n.d). SSHA information is derived from the Global Ocean Physics Analysis and Forecast Daily database from the Copernicus Marine Physics 2D Daily Mean Fields from GEE.

It provides Global Daily Averaged Ocean Surface and variables at the bottom with an 8 km resolution. The forecasts are updated daily, and the parameters from the top to the bottom of the oceans are provided (Fu et al., 2023; Google Earth Engine, 2025). The information generated through cloud computing was mapped and tabulated for further computations through Python libraries. Statistical methodology was applied to this database to generate information on trends in SST and SSHA.

A study of cyclone dynamics can be more validated via multiple methods, in which statistical, interpretive, time-series and causality techniques help in distinguishing noise and also help in generating a clearer picture of short-term variability of the phenomena. The SST, SSHA and cold wake dynamics related to Cyclone Mocha have been subjected to a robust methodology of Pearson's correlation (Borradaile, 2013; Thorand, 2022), Linear Trends, cross correlation function (CCF), Granger Causality (Salvatore & Reagle, 2002) and Z-score transformation (Chatfield, 2003; Salvatore & Reagle, 2002; Telford et al., 1990) for the whole period under SST and SSHA.

Through Pearson's correlation, the SST and SSH levels are recorded in correlation to each other; whether SST coincides with sea level depressions, which is an expected signature of cold wakes. The cooling of the upper ocean and subsequent depression in the sea level via upwelling and thermocline shoaling, as discussed earlier, are considered to be the main drivers behind this.

Linear trends quantify ocean cooling with SSHA and are supposed to indicate temporal changes. The technique is adopted here as a first-order diagnostic tool for the validation of established oceanic responses to TCs. The directionality of this correlation is observed through the study of Granger Causality Analysis, which is based on the assumption that physical mechanisms can have directionality. Is SSHA preceding SST cooling and causing depressions and vice versa? Lagged predictors are used to examine which variable 'leads' to the other statistically.

The details of the techniques applied can be seen in Table 2.

3. Results

The investigation derives its results from a baseline of 15th April to 1st May'23 and extends this analysis to a total duration from 15th April to 31st May'23 to get a broader picture from the results, taking this same baseline period.

3.1. Cold wake analysis

Mocha track, its geographical co-ordinates and meteorological parameters, as visible in Fig. 2 and Table 1, shows the extent and the gradual development of the TC. Buffering of the analysis for a zone of 300 km along Mocha's track, against the baseline of 15th April–1st May' 23, provided distinct and near-real time information of the phenomena under investigation. Figs. 3 and 4 reflect the evolution, development, and dissipation trend of cold wake for the TC. A threshold of ≤–0.5°C was applied to identify an area under the cold wake due to the TC. In its totality, the SST anomaly curve exhibits two distinct phases of cooling in the BoB Fig. 3 plots these. However, the April cooling phase, as exhibited in the graph, is a consequence of pre-monsoonal activity rather than cyclonic circulation. But the intense cooling during the phase of Mocha is a clear indicator of the classic cold wake induced by the TC advancement and landfall.

In the process, strong winds, upwelling and vertical mixing can be attributed to leading the development of a cold wake and SSHA. As indicated by OISST-derived data, Table 3 indicates that in the early stages of Mocha (9th–11th May), the cold wake is relatively small in area. It expands dramatically

Table 2

Details and applicability of statistical techniques used

Method	Formula	Purpose in general	Purpose in study
Pearson's correlation	$r = \Sigma[(X - \bar{X})(Y - \bar{Y})]/\sqrt{(\Sigma(X - \bar{X})^2 \cdot \Sigma(Y - \bar{Y})^2)}$	Linear association between two variables	Strength and direction of SST–SSHA coupling; evaluate how SST cooling aligns with SSHA changes ($r \approx 0.426$, $p = 0.001$)
Linear trend (Regression slope)	Slope = $(y_2 - y_1)/(x_2 - x_1)$	Rate of change over time	Daily SST warming (0.00783°C/day) and SSHA rebound (0.00034 m/day) after the cyclone
CCF	CCF(τ) = Σ(X_t · Y_{t−τ})/(m · σ_X · σ_Y)	Lag relationships between time series	Whether SSHA responds to SST with a lag (SST leads SSHA by ~1–3 days)
Granger causality test	F = ((SSR_r − SSR_ur)/m)/(SSR_ur/(N − k))	Predictive influence of past values	Whether past SST improves the prediction of SSHA (SST → SSHA significant at lags 1–3)
Z-score standardization	$Z = (x - \mu)/s$	Raw values into standardized anomalies	Extreme cold-wake SST anomalies and comparing their magnitude against weaker SSHA Z-scores

Source: Author (2025).
CCF, cross-correlation function; SSR, sum of squared residuals. SST, sea surface temperature.

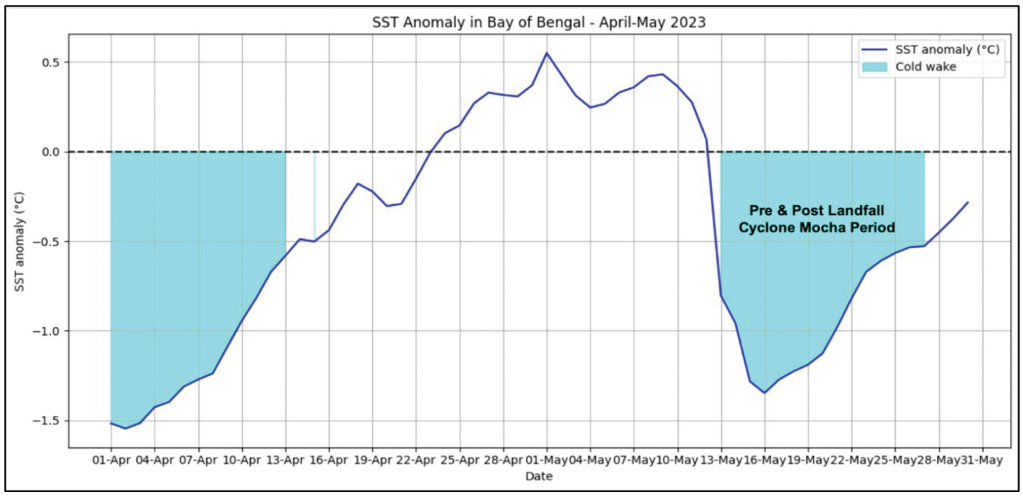

Figure 3

SST anomalies associated with cyclone Mocha. *Source:* Author, 2025 from NOAA/CDR/OISST/V2_1 from GEE. GEE, Google Earth Engine; SST, sea surface temperature.

Table 3

Day-to-day cold wake area under cyclone Mocha

Date	Cold-wake area (km²)
09-05-2023	136,504.40
10-05-2023	170,668.02
11-05-2023	198,361.48
12-05-2023	309,050.11
13-05-2023	622,842.76
14-05-2023	624,954.41
15-05-2023	810,527.85

Source: Author, 2025 from NOAA/CDR/OISST/V2_1 from GEE.
GEE, Google Earth Engine.

with the cyclone's intensification to Category 4 and 5 and reaches approximately to >0.6 million · km² from slightly >0.3 million · km². The observations confirm the existence of a very strong cold wake in terms of intensity and area. Further, the wake gains strength in terms of its area after the landfall of Mocha till 19th May.

As is expected, area under SST anomaly is constantly increasing with the advancement of Mocha for its period from 9th May onwards.

It can be seen that during the cyclone period, a strong and intense cold wake coverage is visible. The maximum area recorded under this is around 0.8 million km². It is derived from the logic that each

OISST grid has an approximate extent of 0.25° × 0.25° (~770 km^2). The multiplication of pixel count by cell area provides the true geography of cold wake area. The details can be interpreted from Fig. 4.

The spatial extent of the cold wake along the Mocha track is supportive of its intensity Fig. 5 shows the pattern of an intensified cooling, established further when examined against the baseline period.

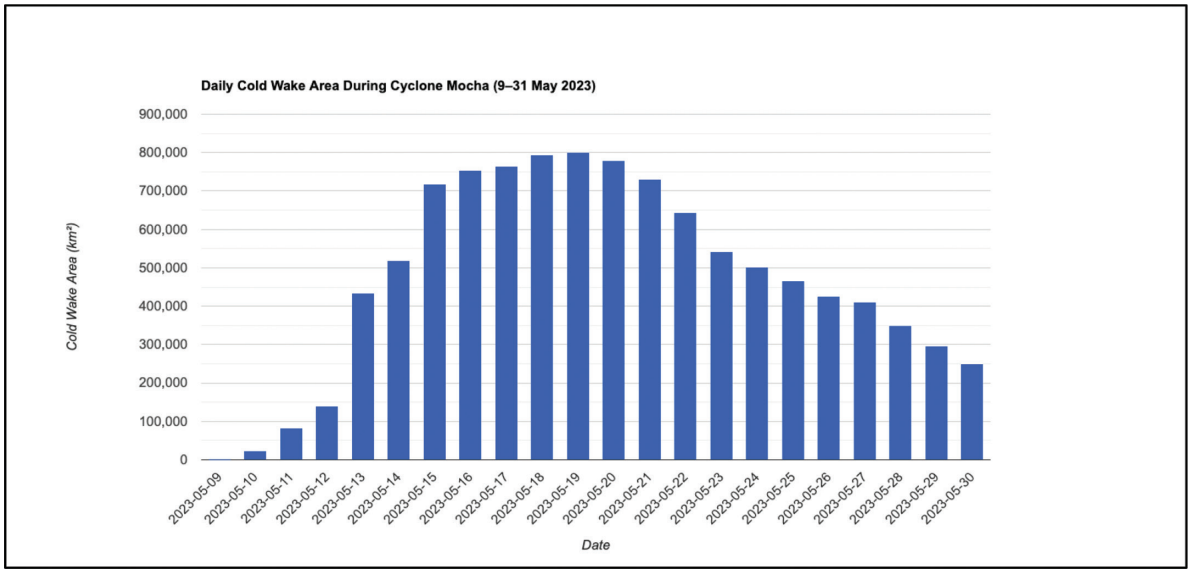

Figure 4

Day wise total area observed under cold wake for cyclone Mocha track in BoB. *Source*: Author, 2025 from NOAA/CDR/OISST/V2_1 from GEE. BoB, Bay of Bengal; GEE, Google Earth Engine.

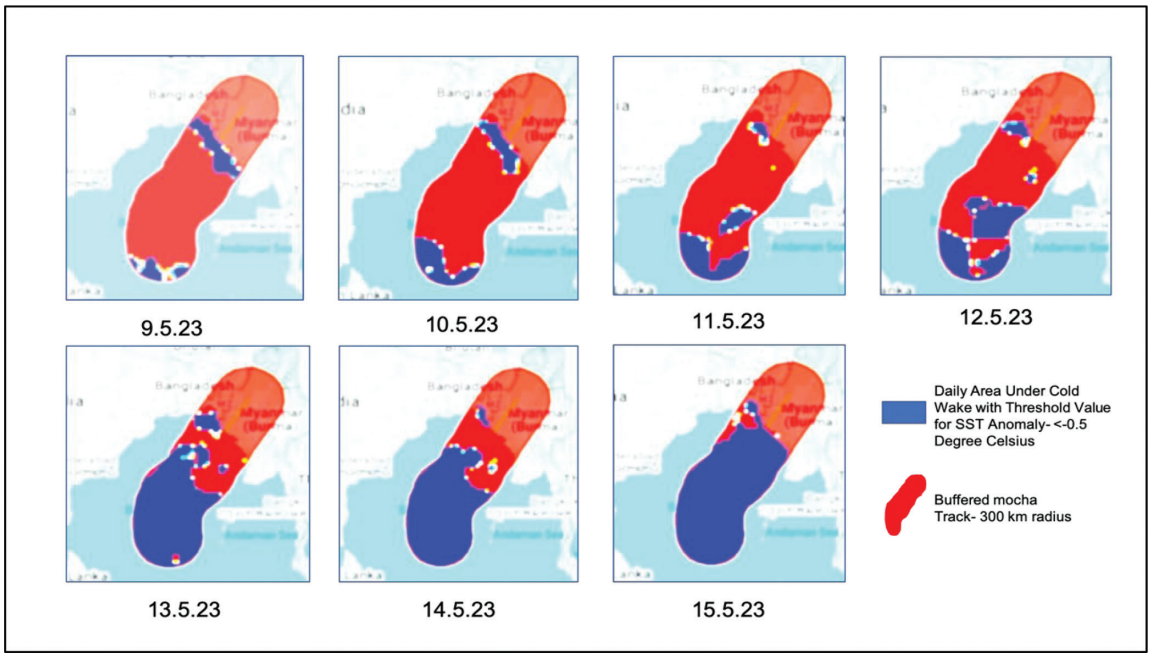

Figure 5

Spatio-temporal extent of cold wake by cyclone Mocha (9th–15th May'23) against the baseline period (15th April–1st May'23). *Source*: Author, 2025 from NOAA/CDR/OISST/V2_1 from GEE. GEE, Google Earth Engine.

Scattering of the initial geographic extent of the cold wake with an SST anomaly of range −0.5°C to −1°C is in synchronicity with the initial development of the cyclone in the southern BoB. The spatial fragmentation starts to fade with the wind speeds picking up intensity and the cyclone's advancement. The band of cooling along the buffer of the TC track is expansive, with the cold wake gaining strength and SST anomalies becoming more prominent.

This sharp increase in cold wake is from 12th to 13th May and is supported spatially and temporally in the direction of the cyclone from Figs. 4 and 5. This enhances further till the landfall on 15th May, with the spatial extent of the cold wake covering the whole of the TC track. The widespread anomalies in SST can be recorded up to −2°C as is visible from Fig. 6.

The anomaly curve clearly establishes a major cooling in the BoB in mid- May, and it is mainly cyclone-driven. Besides, this variability is visible enough to be identified as a strong cyclone Mocha-induced cold wake. Mocha as a TC was unprecedented in the aspect as per records and observations and the findings support the fact.

3.2. SSHA analysis

The spatial and temporal upper ocean dynamic height changes due to Mocha have been depicted in Figs 6. and 7 respectively. The initial negative anomalies (~ −0.01 m to −0.02 m) in April are followed by a falling SSHA, with values at around −0.025 m towards later part of April. These are an indicator of cooler waters closer to the surface. As per oceanographic principles, this is an indicator of a shallow thermocline.

With the further advancement of time in April, anomalies turn to near zero and start becoming positive, indicating an increased water surface of the BoB. A sharper negative anomaly is observed in mid-May during the cyclone, which coincides with Mocha's peak intensity period and later landfall. Cyclone-driven strong mixing, wind stress, and cyclone-driven upwelling are postulated to bring cooler waters to the surface. This sends the SSHA back to near zero and decline, which clearly corresponds with the cold wake signature of the TC.

However, these changes are not very sharp as in other oceans due to the tropical location of the BoB.

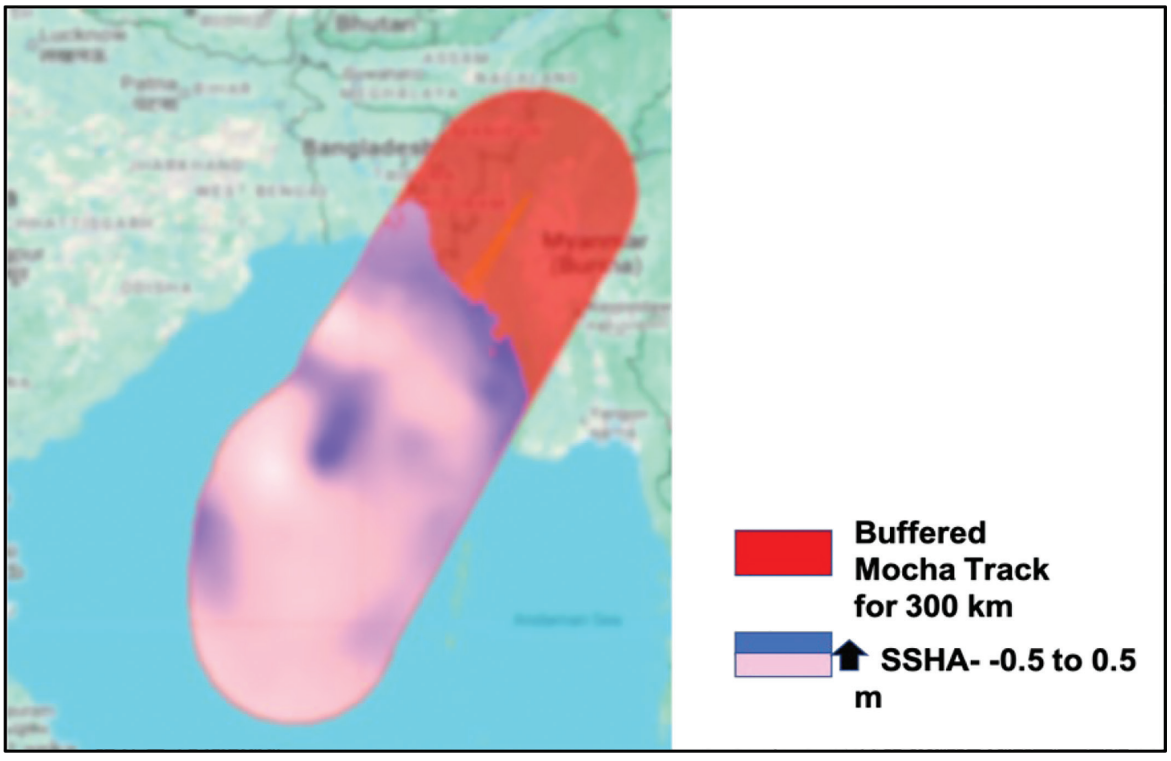

Figure 6

SSHA day-to-day spatial observations for Mocha (9th–15th May'23) against baseline of 15th April–1st May'23. *Source*: Author, 2025 from Copernicus Marine Physics 2D daily mean fields from GEE. GEE, Google Earth Engine.

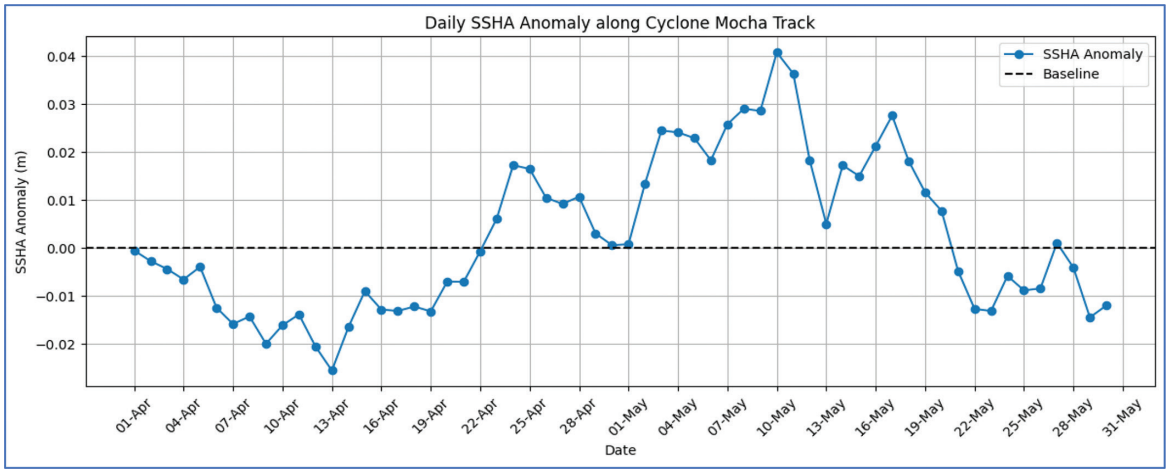

Figure 7

SSHA day-to-day temporal observations for Mocha against baseline of 15th April–1st May'23.

Source: Author, 2025, Derived from NOAA/CDR/OISST/V2_1 from GEE. GEE, Google Earth Engine.

A coherent pattern of pre-cyclone SSHA fall, build-up of upper ocean heat, cyclone-induced falling SSHA and a slow recovery are all visible in Figs. 6 and 7. After Mocha passes, SSHA stabilizes in the −0.01 to −0.02 m range. This is a clear indicator of slow recovery and the vast expanse of the cold wake area.

A multi-parameter time series study of SST and SSHA is shown in Fig. 8. Plotted with demarcating phases for the cyclone from pre-, during, and post-cyclone phases, the figure attempts to provide a holistic view of the thermal and dynamic components of ocean response due to Mocha. A gradual warming from around ~29.5°C toward ~30.5°C is observed in April as a normal feature of the BoB. Strong isolation and weak tropical winds with enhanced SSH and SST also indicate an increased ocean heat content. This leads to positive SSH and SST anomalies. All these conditions also favor the development of the TC.

Table 4. Statistical relationship between SST and SSHA for Cyclone Mocha. However, the formation and advancement of the cyclone causes a sudden turn in observed trends with the SST and SSH declining as a response to Mocha. The divergent trend of both parameters arises out of intense vertical mixing and the entry of cooler water to the subsurface. All this happening within a short interval shows the intensity and strength of Mocha as a TC. This is further supported by the area under the cold wake and also by SSH, which is recorded as taking time to recover. SST tends to re-coup relatively faster, but the impact of the cyclone makes it delayed for the ocean structure from attaining the pre-cyclonic conditions faster. Although the cyclone did produce central upwelling and downwelling, the net impact was rather small. Pre-existing eddies, steric and barotropic elements can also be considered to be operating simultaneously in averaging out SSHA changes. Since the variations in SSHA are not exhibiting large differences along the track, a daily examination is avoided.

3.3. Statistical observations on cold wake, SST, and SSHA

The statistical analysis shown in Table 4 is supportive of the fact that Mocha induced upper ocean thermal and physical changes and also showed an interaction between SST and SSHA. SST was recorded at a maximum of 30.26°C and declined to around 29.73°C during the post cyclone phase. SSHA exhibited a small decline during this period, largely due to Ekman Pumping and cyclone-induced divergence. Pearson correlation value of 0.426 with $p = 0.001$, is indicative of a moderate and statistically significant positive relationship between SST and SSHA.

This denotes that higher SST values tend to coincide with higher sea-level anomalies. Thermal expansion and stratification of upper ocean layers are supported by this finding. The linear trends identify slight increases through the month. SSHA increases by 0.00034 m/day, and SST increases by 0.00783°C/day, although cyclone passage causes brief deviations. These trends show background seasonal warming and gradual dynamical height changes. A rapid oceanic re-stratification is indicated by sea level recovery, as is shown by SSHA. The F-statistic show significance at lag 1–3, which indicates that SST change preceded as well as helps in predicting SSHA variations.

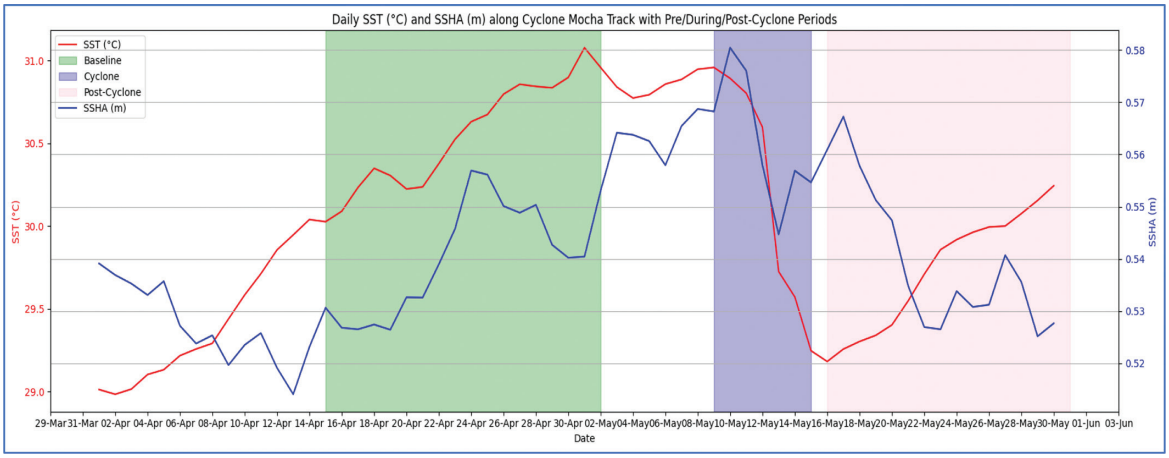

Figure 8

SST and SSHA via baseline for cyclone Mocha. *Source*: Author (2025). SST, sea surface temperature.

Table 4

Statistical relationship between SST and SSHA for cyclone Mocha

Parameter	Value observed	Interpretation
Correlation (SST vs SSHA)	$r = 0.426$, $p = 0.001$	Moderate, significant positive relationship, increase in SST is associated with increase in SSHA.
Linear trend/day (Regression Slope)	SSHA slope: 0.00034 m/day SST slope: 0.00783°C/day	To observe the rate of change between the two parameters
Baseline SSHA	0.081 m	Normal pre-cyclone SSH.
Cyclone-period SSHA	0.078 m	Slight drop, indicating initial setup + partial surge dissipation.
Post-cyclone SSHA	0.0814 m	Returns close to baseline with a rapid recovery of sea level.
Baseline SST	29.54°C	Warm pre-cyclone ocean; fuels cyclone intensification.
Cyclone-period SST	29.09°C	Noticeable drop with a strong cold wake formation
Post-cyclone SST	29.52°C	Re-warming shows restoration of surface stratification.
SSHA trend (post-cyclone)	0.00034 m/day	Very slow increase; structural ocean recovery.
SST trend (post-cyclone)	0.00783°C/day	Stronger warming trend; aligns with rapid recovery of thermal layer.
Granger causality (does SST cause SSHA?)	Significant at lags 1–3	SST changes precede and help predict SSHA variations as thermal forcing influences water column structure.
Z-score anomaly comparison	SST shows larger deviations than SSHA	Cyclone affects temperature more strongly than sea level.
Cold wake intensity (overall track)	~0.45°C cooling	Typical for BoB cyclones; confirms mixing-induced cooling.
Maximum cold wake SST cooling	≈ –1.5°C	Strongest localized SST drop observed in anomaly maps, typically on the right-hand side of the cyclone track where upwelling and mixing are highest.

BoB, Bay of Bengal; SSH, sea surface height; SST, sea surface temperature.

The CCF study indicates that SST anomalies are leading to SSHA changes by 1–3 days. This is an indicator that cyclone-induced surface cooling and mixing precede sea level height adjustments. SST plays a particular role in delaying SSHA changes during the cold wake, which is a confirmation that the sequence of events in the positive lag is from thermodynamic to dynamic factors. The Granger causality tests provide the most important insight across lag orders 1–3, where p-values consistently fall below 0.05, indicating that SST statistically 'Granger-causes' SSHA. Short-term changes in SST help predict subsequent changes in SSHA, suggesting a mechanism where warming or cooling of surface waters leads to density-driven adjustments in SSH. Although complex in real terms, the statistical results strongly support that thermal

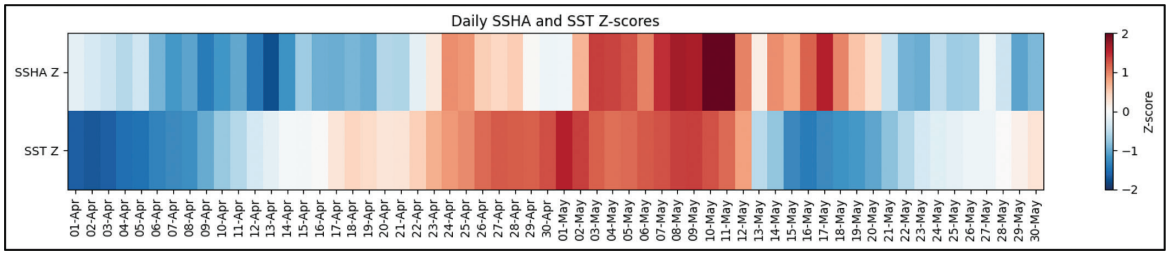

Figure 9

Z-score for SST and SSHA observed for cyclone Mocha (15th April–31st May'23). *Source*: Author (2025). SST, sea surface temperature.

variations precede and influence ocean responses during the cyclone period. Table 4. shows the findings.

The time period and response of SST and SSHA are attempted to be summarized through Z score analysis shown in Fig. 9. The SST Z score band shows an intense transformation toward intense negative anomalies. As cooling due to Mocha's intensification and advancement proceeds northwards, between 14th and 18th May, a pronounced cold wake is observed. This is attributed mainly to wind intensity, upwelling and mixing. SST tends to gain 'normalcy' around the end of the month. SSHA is showing a more subdued pattern. As detailed earlier, the negative anomalies assume positive values with the cyclone. However, a slight aspect in this, which can be added to cyclonic convergence, is the fact that there might be a probability of the cyclone passing over a comparatively elevated water surface. The Z- score map indicates SST responding rapidly and strongly, while SSHA is weaker with a more controlled behavior. These are indicators of distinct physical and thermal processes operating in the BoB.

4. Discussions

The cold wake generated by TCs presents important insights to oceanological and meteorological research. Mocha holds implications in the context of its unprecedented nature as a TC in the BoB. Computing generated a sharp fall in SST by Mocha and a strong cold-wake, which persisted for a couple of days after the passage of the TC. It also probably created negative feedback loops, which seem to reduce subsequent convective activity and suppress potential cyclogenesis in the BoB as the cold wake subsided.

This could also have impacted and have been affected by pre and monsoonal dynamics as SSTs are pivotal in monsoon convection, winds and precipitation. Understanding such wake dynamics is helpful for climatological research. High resolution remote sensing, such as the one applied in the current study, is highlighted as a powerful tool in analysis of TCs (Ali et al., 2011; Cheung et al., 2013; Cione et al., 2013; Kerhalkar et al., 2025; Mei et al., 2015; Ricciardulli et al., 2023; Zhao et al., 2022). A dominant SST cooling observed in the right-hand quadrant of Cyclone Mocha's track is in alignment with established cyclone-ocean interaction dynamics in the Northern Hemisphere.

The stronger wind stress and the additive effect of the cyclone's motion and rotation result in an enhanced mixing, Ekman divergence, with an enhanced upwelling of cooler subsurface waters, contributing to a more intense cold wake (Akhila et al., 2022; Chu et al., 2000; Dickey et al., 1998; Kerhalkar et al., 2025; Oey et al., 2007; Price, 1981; Sala et al., 2024; Shetye et al., 1996; Wang et al., 2016, 2024). Sea surface depression can be attributed to thermocline shoaling and vertical displacement of water masses induced by wind-forced upwelling (Shay et al., 2000). These anomalies show the significant role of cyclone kinematics in modifying oceanic response. They also explain the spatial dynamics of ocean anomalies trailing TCs' passage. Cold wakes and SSH anomalies arising out of small- and large-scale meteorological phenomena also help in nutrient uplift, which may trigger phytoplankton blooms post TC (Kumar et al., 2024; Lin et al., 2003; Maneesha et al., 2011; Vinayachandran & Mathew, 2003; Walker et al., 2005), though not explored in this study.

The cold wake, SST, and SSH anomaly trend around Cyclone Mocha provide insights into how short-term ocean responses occur. The findings have been facilitated by the selection of the baseline period. Gradually, strong and persistently rising SST anomalies and their sustenance for a couple of days indicate the strength of the cyclone. A further gradual rise in temperature shows a warm ocean surface consistent either with the anthropocene rise in global SSTs (Kang & Moon, 2022; Ridderinkhof et al., 2010; Webster

et al., 2005) and/or also due to pre-monsoonal conditions in the BoB (Alam et al., 2003; Busireddy et al., 2019; Subbaramayya and Rao, 1984).

Since all anomalies were calculated with respect to an immediate baseline, the results provide an extended response of the ocean to Cyclone Mocha. Besides, the role of 'other' factors can also be negated with this timeline. So, the outcomes are more validated and supportive of the existence of a strong cold wake with the intense TC (John et al., 2025; Karnauskas et al., 2021; Kuttippurath et al., 2022; Ling et al., 2021). The study also supports variation of SSH with changes in SST (Feng, 2012; Ji et al., 2021; Novi & Bracco, 2021; Oey et al., 2007).

The right-hand side stronger cooling is observed in the Northern Hemisphere for TCs, a feature commonly attributed to enhanced Ekman pumping and wind stress curl in the Northern Hemisphere (Mishra et al., 2024; Price et al., 1994; Singh & Roxy, 2022; Wang et al., 2016). Thus, recovery may extend 10–20 days, compared to the typical 3–7 days in less stratified basins (Chacko & Jayaram, 2022; Navaneeth et al., 2019; Shenoi et al., 2002). They can also reduce subsequent storm intensity by lowering SSTs (Karnauskas et al., 2021).

Surface cooling accompanied by cold wakes after the passage of TCs in the BoB is recorded as bringing a significant decline in surface temperatures of the waters. In this category, pre-monsoon cyclones have more capacity to cause stronger cold wakes as compared to post-monsoon TCs (Kuttippurath et al., 2022). Intense cooling is consistent with previous strong cyclonic events over the BoB as reported (Vissa et al., 2013). However, the recovery of SST anomalies may be consistent with the BoB's warmer conditions reported in recent regional studies suggesting climate-induced amplification of oceans and TCs along the impacts of ocean heat, El Nino and Southern Oscillation, Madden Julian Oscillation and Indian Ocean Dipole (Alamgir et al., 2025; Albert & Bhaskaran, 2020; Bhardwaj et al., 2019; Bhatia et al., 2019; John et al., 2025; McNeil & Matear, 2008; Selva et al., 2025).

The recovery form SST cooling is also indicative of regional ocean dynamics (Ji et al., 2021; John et al., 2025; Ling et al., 2021). Each TC is unique, and (Chacko & Jayaram, 2022) and Mocha also serves as a critical case study for analyzing how large-scale atmospheric disturbances interact with regional oceanography in one of the world's most cyclone-prone marine environments.

5. Conclusions

The current attempt is a contribution to the literature on oceanographic studies in the light of observations of regional ocean dynamics and aspects evolving with climate change in hindsight. It validates and supports typical ocean response to TCs as reflected in SST changes, cold wakes, SSH anomalies and regional hydrology. While it was based on the assumption of the complexity of TCs and related ocean dynamics, it managed to derive outcomes through databases, which can be said to be a strong support in deriving information on the inaccessible dimensions of hydro-meteorological studies. The use of remote sensing-derived information and high-resolution databases is in consonance with the recent developments in the field. The detailed statistical responses drawn support existing literature and also contribute to TC research. The results collectively confirm that Cyclone Mocha produced a rapid thermal response and a weaker, delayed dynamical adjustment in the BoB as reflected through SST and SSHA, respectively. The topic lends insights into TCs and ocean responses, particularly on Mocha, which are evolving.

Declaration

The author declares no potential conflicts of interest. This study was conducted independently, without any financial or personal relationships that could influence the findings. All interpretations and conclusions are solely those of the author, based on objective analysis.

References

Akhila, R. S., Kuttippurath, J., Chakraborty, A., Sunanda, N., & Peter, R. (2025). Rapid intensification of the Super Cyclone Amphan: Environmental drivers and its future projections. *Tropical Cyclone Research and Review, 14*(1), 27–39. https://doi.org/10.1016/j.tcrr.2025.02.005

Akhila, R. S., Kuttippurath, J., Sarojini, B. B., Chakraborty, A., & Rahul, R. (2022). Observed tropical cyclone-driven cold wakes in the context of rapid warming of the Arabian Sea. *Tellus A: Dynamic Meteorology and Oceanography, 74*(1), 236–251. https://doi.org/10.1080/16000870.2022.2072646

Alamgir, M., Hashim, M., Pour, A. B., & Shahid, S. (2025). Transformation in the sea surface properties of the Bay of Bengal under climate change. *Ocean Dynamics, 75*, Article 76. https://doi.org/10.1007/s10236-025-01715-1

Alam, M. M., Hossain, M. A., & Shafee, S. (2003). Frequency of Bay of Bengal cyclonic storms and depressions crossing different coastal zones. *International Journal of Climatology, 23*(9), 1119–1125. https://doi.org/10.1002/joc.927

Albert, J., & Bhaskaran, P. K. (2020). Ocean heat content and its role in tropical cyclogenesis for the Bay of Bengal basin. *Climate Dynamics, 55*(11–12), 3343–3362. https://doi.org/10.1007/s00382-020-05450-9

Ali, M. M., Goni, G. J., & Jayaraman, V. (2011). Satellite-derived ocean heat content improves cyclone predictions: Utilization of satellite-derived oceanic heat content for cyclone studies, Hyderabad, India, 25–26 March 2010. *Eos, Transactions American Geophysical Union, 92*(43), 357–358. https://doi.org/10.1029/2010EO430009

Balaguru, K., Chang, P., Saravanan, R., Leung, L. R., Xu, Z., Li, M., & Hsieh, J.-S. (2012). Ocean barrier layers' effect on tropical cyclone intensification. *Proceedings of the National Academy of Sciences of the United States of America, 109*(36), 14343–14347. https://doi.org/10.1073/pnas.1201364109

Bernier, N. B., Hemer, M., Mori, N., Appendini, C. M., Breivik, O., de Camargo, R., Casas-Prat, M., Duong, T. M., Haigh, I. D., Howard, T., Hernaman, V., Huizy, O., Irish, J. L., Kirezci, E., Kohno, N., Lee, J.-W., McInnes, K. L., Meyer, E. M. I., Marcos, M., … Zhang, Y. J. (2024). Storm surges and extreme sea levels: Review, establishment of model intercomparison and coordination of surge climate projection efforts (SurgeMIP). *Weather and Climate Extremes, 45*, 100689. https://doi.org/10.1016/j.wace.2024.100689

Bhardwaj, P., Singh, O., Pattanaik, D. R., & Klotzbach, P. J. (2019). Modulation of Bay of Bengal tropical cyclone activity by the Madden–Julian Oscillation. *Atmospheric Research, 229*, 23–38. https://doi.org/10.1016/j.atmosres.2019.06.010

Bhatia, K. T., Vecchi, G. A., Knutson, T. R., Murakami, H., Dixon, K. W., & Whitlock, C. E. (2019). Recent increases in tropical cyclone intensification rates. *Nature Communications, 10*(1), 635. https://doi.org/10.1038/s41467-019-08471-z

Borradaile, G. J. (2013). Statistics of earth science data: Their distribution in time, space and orientation. Springer Berlin Heidelberg.

Busireddy, N. K. R., Ankur, K., Osuri, K. K., Sivareddy, S., & Niyogi, D. (2019). The response of ocean parameters to tropical cyclones in the Bay of Bengal. *Quarterly Journal of the Royal Meteorological Society, 145*(724), 3320–3332. https://doi.org/10.1002/qj.3622

Chacko, N., & Jayaram, C. (2022). Response of the Bay of Bengal to super cyclone Amphan examined using synergistic satellite and in-situ observations. *Oceanologia, 63*(4), 493–505. https://doi.org/10.1016/j.oceano.2021.09.006

Chatfield, C. (2003). *The analysis of time series: An Introduction* (6th ed.). CRC Press.

Cheng, X., Xie, S.-P., McCreary, J. P., Qi, Y., & Du, Y. (2013). Intraseasonal variability of sea surface height in the Bay of Bengal. *Journal of Geophysical Research: Oceans, 118*(1), 1–15. https://doi.org/10.1002/jgrc.20075

Cheung, H.-F., Pan, J., Gu, Y., & Wang, Z. (2013). Remote-sensing observation of ocean responses to Typhoon Lupit in the northwest Pacific. *International Journal of Remote Sensing, 34*(4), 1478–1491. https://doi.org/10.1080/01431161.2012.721940

Chu, P. C., Veneziano, J. M., Fan, C., Carron, M. J., & Liu, W. T. (2000). Response of the South China Sea to tropical cyclone Ernie (1996). *Journal of Geophysical Research: Oceans, 105*(C6), 13991–14009. https://doi.org/10.1029/2000JC900035

Cione, J. J., Kalina, E. A., Zhang, J. A., & Uhlhorn, E. W. (2013). Observations of air–sea interaction and intensity change in hurricanes. *Monthly Weather Review, 141*(7), 2368–2382. https://doi.org/10.1175/MWR-D-12-00070.1

Cione, J. J., & Uhlhorn, E. W. (2003). Sea surface temperature variability in hurricanes: Implications with respect to intensity change. *Monthly Weather Review, 131*(8), 1783–1796. https://doi.org/10.1175/2562.1

D'Asaro, E., Lee, C., Rainville, L., Harcourt, R., & Thomas, L. (2011). Enhanced turbulence and energy dissipation at ocean fronts. *Science, 332*(6027), 318–322. https://doi.org/10.1126/science.1201515

Dare, R. A., & McBride, J. L. (2011). Sea surface temperature response to tropical cyclones. *Monthly Weather Review, 139*(12), 3798–3808. https://doi.org/10.1175/MWR-D-10-05019.1

Das, G. K., & Debnath, G. C. (2017). Governing factors associated with intensification of TC—A diagnostic study of VSCS Phailin and Lehar. In M. Mohapatra, B. Bandyopadhyay, & L. Rathore (Eds.), *Tropical cyclone activity over the North Indian Ocean* (pp. 245–255). Springer. https://doi.org/10.1007/978-3-319-40576-6_17

Das, R., Mondal, S., Mandal, A. K., Jaiswal, N., Saha, T. K., & De, T. K. (2025). Study of Bay of Bengal cyclones for year 2023 using SCAT-3 and GFS datasets and numerical simulation of associated surges using SWAN + ADCIRC model. *Ocean Dynamics, 75*, 74. https://doi.org/10.1007/s10236-025-01722-2

Dickey, T., Frye, D., McNeil, J., Manov, D., Nelson, N., Sigurdson, D., Jannasch, H., Siegel, D., Michaels, A., & Johnson, R. (1998). Upper-ocean temperature response to Hurricane Felix as measured by the Bermuda Testbed Mooring. *Monthly Weather Review, 126*(5), 1195–1201. https://doi.org/10.1175/1520-0493(1998)126<1195:UOTRTH>2.0.CO;2

Dube, S. K., Jain, I., Rao, A. D., & Murty, T. S. (2009). Storm surge modelling for the Bay of Bengal and Arabian Sea. *Natural Hazards, 51*(1), 3–27. https://doi.org/10.1007/s11069-009-9397-9

Elizabeth, A. I., Effy, J. B., & Francis, P. A. (2020). On the upper ocean response of Bay of Bengal to very severe cyclones Phailin and Hudhud. *Journal of Operational Oceanography, 15*(1), 17–31. https://doi.org/10.1080/1755876X.2020.1813412

Emanuel, K. A. (1986). An air-sea interaction theory for tropical cyclones. Part I: Steady-state maintenance. *Journal of the Atmospheric Sciences, 43*(6), 585–604. https://doi.org/10.1175/1520-0469(1986)043<0585:AASITF>2.0.CO;2

Feng, J. Q. (2012). Interannual coherent variability of SSTA and SSHA in the Tropical Indian Ocean. *Ocean Science Discussions, 9*(1), 1–24. https://doi.org/10.5194/osd-9-1-2012

Fu, H., Dan, B., Gao, Z., Wu, X., Chao, G., Zhang, L., Zhang, Y., Liu, K., Zhang, X., & Li, W. (2023). Global ocean reanalysis

CORA2 and its inter comparison with a set of other reanalysis products. *Frontiers in Marine Science, 10*, 1084186. https://doi.org/10.3389/fmars.2023.1084186

Goni, G. J., & Trinanes, J. A. (2011). Ocean thermal structure monitoring could aid in the intensity forecast of tropical cyclones. *Eos, 92*(51), 247–248. https://doi.org/10.1029/2003EO510001

Google Earth Engine. (2025). *Google Earth Engine Code Editor*. https://code.earthengine.google.com/

Gopalan, A. K. S., Gopala Krishna, V. V., Ali, M. M., & Sharma, R. (2000). Detection of Bay of Bengal eddies from TOPEX and in situ observations. *Journal of Marine Research, 58*(5), 721–734. https://doi.org/10.1357/002224000321358873

IMD. (2023). *Tropical cyclone mocha report*. India Meteorological Department.

INCOIS. (2023). *Post-cyclone mocha SST and SSH analysis report*. Indian National Centre for Ocean Information Services. https://incois.gov.in.

Jarugula, S. L., & McPhaden, M. J. (2022). Ocean mixed layer response to two post-monsoon cyclones in the Bay of Bengal in 2018. *Journal of Geophysical Research: Oceans, 127*(9), e2022JC018874. https://doi.org/10.1029/2022JC018874

Ji, C., Zhang, Y., Cheng, Q., & Tsou, J. Y. (2021). Investigating ocean surface responses to typhoons using reconstructed satellite data. *International Journal of Applied Earth Observation and Geoinformation, 103*, 102474. https://doi.org/10.1016/j.jag.2021.102474

John, E. B., Balaguru, K., Leung, L. R., Foltz, G. R., & Hagos, S. M. (2025). Faster recovery of North Atlantic tropical cyclone-induced cold wakes in recent decades. *npj Climate and Atmospheric Science, 8*, Article 188. (osti.gov). https://doi.org/10.1038/s41612-025-01029-5

Jourdain, N. C., Lengaigne, M., Vialard, J., Madec, G., Menkes, C. E., Vincent, E. M., Jullien, S., & Barnier, B. (2013). Observation-based estimates of surface cooling inhibition by heavy rainfall under tropical cyclones. *Journal of Physical Oceanography, 43*(1), 205–221. https://doi.org/10.1175/JPO-D-12-085.1

JTWC. (2023). *Tropical cyclone mocha warning bulletins*. Joint Typhoon Warning Center.

Kang, K., & Moon, I.-J. (2022). Sea surface height changes due to the tropical cyclone-induced water mixing in the Yellow Sea, Korea. *Frontiers in Earth Science, 10*, Article 826582. https://doi.org/10.3389/feart.2022.826582

Karnauskas, K. B., Zhang, L., & Emanuel, K. A. (2021). The feedback of cold wakes on tropical cyclones. *Geophysical Research Letters, 48*(7), e2020GL091676. https://doi.org/10.1029/2020GL091676

Kerhalkar, S., Kannad, A., Kinsella, A., Tandon, A., Sprintall, J., & Lee, C. M. (2025). Monsoon-frontal interactions drive Cyclone Biparjoy's wake recovery in the Arabian Sea. *Geophysical Research Letters, 52*(4), e2024GL112413. https://doi.org/10.1029/2024GL112413

Kodunthirapully Narayanaswami, N., & Ramasamy, V. (2022). Tropical cyclone intensity modulated by the oceanic eddies in the Bay of Bengal. *Oceanologia, 64*(2), 257–270. https://doi.org/10.1016/j.oceano.2022.02.005

Kranthi, G. M., Deshpande, M., Sunilkumar, K., Emmanuel, R., & Ingle, S. (2022). Climatology and characteristics of rapidly intensifying tropical cyclones over the North Indian Ocean. *International Journal of Climatology, 43*(2), 1234–1248. https://doi.org/10.1002/joc.7945

Kumar, A., Chakraborty, A., & Sagar, A. K. (2024). Analysis of the Bay of Bengal cyclone and its rejuvenation in the Arabian Sea after passing over peninsular India. *Geomatics, Natural Hazards and Risk, 15*(1), Article 2433110. https://doi.org/10.1080/19475705.2024.2433110

Kuttippurath, J., Akhila, R. S., Martin, M. V., Girishkumar, M. S., Mohapatra, M., Sarojini, B. B., Mogensen, K., Sunanda, N., & Chakraborty, A. (2022). Tropical cyclone-induced cold wakes in the northeast Indian Ocean. *Environmental Science: Atmospheres, 2*(3), 404–415. https://doi.org/10.1039/D1EA00066G

Lin, I. I., Liu, W. T., Wu, C.-C., Wong, G. T. F., Hu, C., Chen, Z., Liang, W.-D., Yang, Y., & Liu, K.-K. (2003). New evidence for enhanced ocean primary production triggered by tropical cyclone. *Geophysical Research Letters, 30*(13), 1718. https://doi.org/10.1029/2003GL017141

Lin, I.-I., Pun, I.-F., & Wu, C.-C. (2009). Upper-ocean thermal structure and the western North Pacific category 5 typhoons. Part II: Dependence on translation speed. *Monthly Weather Review, 137*(11), 3744–3757. https://doi.org/10.1175/2009MWR2713.1

Ling, Z., Chen, Z., Wang, G., He, H., & Chen, C. (2021). Recovery of tropical cyclone–induced SST cooling observed by satellite in the northwestern Pacific Ocean. *Remote Sensing, 13*(18), Article 3781. https://doi.org/10.3390/rs13183781

Lloyd, I. D., & Vecchi, G. A. (2011). Observational evidence for oceanic controls on hurricane intensity. *Journal of Climate, 24*(4), 1138–1153. https://doi.org/10.1175/2010JCLI3763.1

Makarieva, A. M., Gorshkov, V. G., & Li, B.-L. (2008). On the validity of representing hurricanes as Carnot heat engines. *Atmospheric Chemistry and Physics Discussions, 8*, 17423–17437. https://doi.org/10.5194/acpd-8-17423-2008

Maneesha, K., Sarma, V. V. S. S., Reddy, N. P. C., Sadhuram, Y., Ramana Murty, T. V., Sarma, V. V., & Dileep, K. M. (2011). Meso-scale atmospheric events promote phytoplankton blooms in the coastal Bay of Bengal. *Journal of Earth System Science, 120*(4), 773–782. https://doi.org/10.1007/s12040-011-0089-y

McNeil, B. I., & Matear, R. J. (2008). Southern Ocean acidification: A tipping point at 450-ppm atmospheric CO_2. *Proceedings of the National academy of Sciences of the United States of America, 105*(48), 18860–18864. https://doi.org/10.1073/pnas.0806318105

Mei, W., Lien, C.-C., Lin, I.-I., & Xie, S.-P. (2015). Tropical cyclone–induced ocean response: A comparative study of the South China Sea and tropical Northwest Pacific. *Journal of Climate, 28*(15), 5952–5968. https://doi.org/10.1175/JCLI-D-14-00651.1

Mishra, A. K., Jangir, B., & Strobach, E. (2024). Influence of mesoscale sea-surface temperature structures on the Mediterranean cyclone Ianos in convection-permitting simulations: Contributions of surface warming and cold wakes. *Quarterly Journal of the Royal Meteorological Society, 150*(765), 5146–5166. https://doi.org/10.1002/qj.4862

Mittal, R., Tewari, M., Radhakrishnan, C., Ray, P., Singh, T., & Nickerson, A. K. (2019). Response of tropical cyclone Phailin (2013) in the Bay of Bengal to climate perturbations. *Climate Dynamics, 53*(3–4), 2013–2030. https://doi.org/10.1007/s00382-019-04761-w

Mohanty, P. K., Pradhan, Y., Nayak, S. R., Panda, U. S., & Mohapatra, G. N. (2008). Sediment dispersion in the Bay of Bengal. In P. K. Mohanty (Ed.), *Monitoring and modelling lakes and coastal environments* (pp. 50–78). Springer. https://doi.org/10.1007/978-1-4020-6646-7_5

Mukherjee, P., Rajendiran, S., Ravikumar, B. H., & Ramakrishnan, B. (2024). Comparative evaluation of meteorological inputs for improved storm surge modeling: A case study of tropical Cyclone Vayu. *Dynamics of Atmospheres and Oceans, 105*, 101461. https://doi.org/10.1016/j.dynatmoce.2024.101461

Murty, T. S., Flather, R. A., & Henry, R. F. (1986). The storm surge problem in the Bay of Bengal. *Progress in Oceanography, 16*(4), 195–233. https://doi.org/10.1016/0079-6611(86)90039-X

NASA Earth Observatory. (2023, May 14). *Cyclone mocha strikes Myanmar*. https://www.earthobservatory.nasa.gov/images/151343/cyclone-mocha-strikes-myanmar

National Centers for Environmental Information. (n.d.). *Optimum Interpolation Sea Surface Temperature (OISST)*. Retrieved [October 25], from https://www.ncei.noaa.gov/products/optimum-interpolation-sst NCEI+2NCEI+2

Navaneeth, K. N., Martin, M. V., Joseph, K. J., & Venkatesan, R. (2019). Contrasting the upper ocean response to two intense cyclones in the Bay of Bengal. *Deep Sea Research Part I: Oceanographic Research Papers, 147*, 65–78. https://doi.org/10.1016/j.dsr.2019.03.010

Neetu, S., Lengaigne, M., Vincent, E. M., Vialard, J., Durand, F., Madec, G., Samson, G., & Kumar, M. R. R. (2012). Influence of oceanic stratification on tropical cyclone–induced surface cooling in the Bay of Bengal. *Journal of Geophysical Research: Oceans, 117*(C12), C12020. https://doi.org/10.1029/2012JC008433

Nelson, N. B. (1996). Cover: The wake of hurricane felix. *International Journal of Remote Sensing, 17*(15), 2893–2895. https://doi.org/10.1080/01431169608949116

Novi, L., & Bracco, A. (2021). Uncovering marine connectivity through sea surface temperature. *Scientific Reports, 11*(1), Article 87711. https://doi.org/10.1038/s41598-021-87711-z

Oey, L.-Y., Ezer, T., Wang, D.-P., Yin, X.-Q., & Fan, S.-J. (2007). Hurricane-induced motions and interaction with ocean currents. *Continental Shelf Research, 27*(9), 1249–1263. https://doi.org/10.1016/j.csr.2007.01.008

Oginni, T. E., Li, S., He, H., Yang, H., & Ling, Z. (2021). Ocean response to Super-Typhoon Haiyan. *Water, 13*(20), 2841. https://doi.org/10.3390/w13202841

Ortiz, A. M. D., Chua, P. L. C., Salvador, D. Jr., Dacles, T. G., Torres, J. P., & Abesamis, R. A. (2023). Impact of tropical cyclones on food security, health and biodiversity. *Bulletin of the World Health Organization, 101*(2), 152–154. https://doi.org/10.2471/BLT.22.288838

Pasquero, C., Desbiolles, F., & Meroni, A. N. (2021). Air-sea interactions in the cold wakes of tropical cyclones. *Geophysical Research Letters, 48*(2), e2020GL091185. https://doi.org/10.1029/2020GL091185

Pathirana, G., & Priyadarshani, K. (2022). Tropical cyclones in the Arabian Sea and the Bay of Bengal: Comparison of environmental factors. *Journal of the National Science Foundation of Sri Lanka, 50*(1), 53–64. https://doi.org/10.227/jnsfsr.v50i1.10424

Prakash, K. R., & Pant, V. (2020). On the wave-current interaction during the passage of a tropical cyclone in the Bay of Bengal. *Deep Sea Research Part II: Topical Studies in Oceanography, 172*, 104658. https://doi.org/10.1016/j.dsr2.2019.104658

Price, J. F. (1981). Upper ocean response to a hurricane. *Journal of Physical Oceanography, 11*(2), 153–175. https://doi.org/10.1175/1520-0485(1981)011<0153:UORTAH>2.CO;2

Price, J. F. (2009). Metrics of hurricane–ocean interaction: Vertically integrated or vertically averaged ocean temperature? *Ocean Science, 5*(3), 351–368. https://doi.org/10.5194/os-5-351-2009

Price, J. F., Sanford, T. B., & Forristall, G. Z. (1994). Forced stage response to a moving hurricane. *Journal of Physical Oceanography, 24*(2), 233–260. https://doi.org/10.1175/1520-0485(1994)024<0233:FSRTAM>2.0.CO;2

Ramachandran, S., Tandon, A., Mackinnon, J., Lucas, A. J., Pinkel, R., Waterhouse, A. F., Nash, J., Shroyer, E., Mahadevan, A., Weller, R. A., & Farrar, J. T. (2018). Submesoscale processes at shallow salinity fronts in the Bay of Bengal: Observations during the winter monsoon. *Journal of Physical Oceanography, 48*(3), 479–509. https://doi.org/10.1175/JPO-D-16-0283.1

Ren, D., Han, S., & Wang, S. (2024). Upper ocean responses to tropical cyclone Mekunu (2018) in the Arabian Sea. *Journal of Marine Science and Engineering, 12*(7), 1177. https://doi.org/10.3390/jmse12071177

Ricciardulli, L., Howell, B., Jackson, C. R., Hawkins, J., Courtney, J., Stoffelen, A., Langlade, S., Fogarty, C., Mouche, A., Blackwell, W., Meissner, T., Heming, J., Candy, B., McNally, T., Kazumori, M., Khadke, C., & Escullar, M. A. G. (2023). Remote sensing and analysis of tropical cyclones: Current and emerging satellite sensors. *Tropical Cyclone Research and Review, 12*(4), 267–293. https://doi.org/10.1016/j.tcrr.2023.12.003

Ridderinkhof, H., van der Werf, P. M., Ullgren, J. E., van Aken, H. M., van Leeuwen, P. J., & de Ruijter, W. P. M. (2010). Seasonal and interannual variability in the Mozambique Channel from moored current observations. *Journal of Geophysical Research: Oceans, 115*(C6), C06010. https://doi.org/10.1029/2009JC005619

Roxy, M. K., Kapoor, R., Terray, P., & Masson, S. (2014). The curious case of Indian Ocean warming. *Journal of Climate, 27*(22), 8501–8509. https://doi.org/10.1175/JCLI-D-14-00471.1

Sadhuram, Y. (2004). Record decrease of sea surface temperature following the passage of a super cyclone over the Bay of Bengal. *Current Science, 86*(3), 383–384.

Sala, J., Giglio, D., Hu, A., Kuusela, M., Wood, K. M., & Lee, A. B. (2024). Upper-ocean changes with hurricane-strength wind events: A study using Argo profiles and an ocean reanalysis. *Ocean Science, 20*(6), 1441–1455. https://doi.org/10.5194/os-20-1441-2024

Salvatore, D., & Reagle, D. (2002). Schaum's outline of statistics and econometrics. Mcgraw-hill.

Sanford, T. B., Price, J. F., Girton, J. B., & Webb, D. C. (2007). Highly resolved observations and simulations of the ocean response to a hurricane. *Geophysical Research Letters, 34*(13), L13604. https://doi.org/10.1029/2007GL029679

Schade, L. R., & Emanuel, K. A. (1999). The ocean's effect on the intensity of tropical cyclones: Results from a simple coupled atmosphere–ocean model. *Journal of the Atmospheric Sciences, 56*(4), 642–651. https://doi.org/10.1175/1520-0469(1999)056<0642:TOSEOT>2.0.CO;2

Selva, K. M., Geethalakshmi, V., Pazhanivelan, S., Subrahmaniyan, K., Dheebakaran, G. A., Saravanakumar, V., Bhuvaneswari, K., & Pugazenthi, K. (2025). Review on evolving cyclone patterns in Bay of Bengal: Challenges for coastal agriculture. *Plant Science Today, 12*(sp1), 01–11. https://doi.org/10.14719/pst.11369

Sengupta, D., Raj, G. N. B., & Shenoi, S. S. C. (2006). Surface freshwater from Bay of Bengal runoff and Indonesian throughflow in the tropical Indian Ocean. *Geophysical Research Letters, 33*(22), L22609. https://doi.org/10.1029/2006GL027573

Sharma, S., Kumar, A., & Chakraborty, A. (2024). Intensification of heatwave conditions during Cyclone Mocha in 2023. *Weather, 79*(7), 220–223. https://doi.org/10.1002/wea.4553

Shay, L. K., Goni, G. J., & Black, P. G. (2000). Effects of a warm oceanic feature on Hurricane Opal. *Monthly Weather Review, 128*(5), 1366–1383. https://doi.org/10.1175/1520-0493(2000)128<1366:EOAWOF>2.0.CO;2

Shenoi, S. S. C., Shankar, D., & Shetye, S. R. (2002). Differences in heat budgets of the near-surface Arabian Sea and Bay of Bengal: Implications for the summer monsoon. *Journal of Geophysical Research: Oceans, 107*(C6), 3052. https://doi.org/10.1029/2000JC000679

Shetye, S. R., Gouveia, A. D., Shankar, D., Shenoi, S. S. C., Vinaychandran, P. N., Sundar, D., Michael, G. S., & Nampoothiri, G. (1996). Hydrography and circulation in the western Bay of Bengal during the northeast monsoon. *Journal of Geophysical Research, 101*(C7), *14*(011–14), 025. https://doi.org/10.1029/95JC03307

Singh, V. K., & Roxy, M. K. (2022). A review of ocean-atmosphere interactions during tropical cyclones in the north Indian Ocean. *Earth-Science Reviews, 228*, 103967. https://doi.org/10.1016/j.earscirev.2022.103967

Srinivas, C. V., Mohan, G. M., Bhaskar Rao, D. V., Baskaran, R., & Venkatraman, B. (2016). Numerical simulations with WRF to study the impact of sea surface temperature on the evolution of tropical cyclones over Bay of Bengal. *Tropical cyclone activity over the North Indian Ocean* (pp. 259–271). Springer.

Subbaramayya, I., & Rao, S. R. M. (1984). Frequency of Bay of Bengal cyclones in the post-monsoon season. *Monthly Weather Review, 112*(8), 1640–1642. https://doi.org/10.1175/1520-0493(1984)112<1640:FOBOBC>2.0.CO;2

Suda, K. (1943). Kaiyō Kagaku (The science of the sea). Kokin Shoin.

Telford, W. M., Geldart, L. P., & Sheriff, R. E. (1990). *Applied geophysics*. Cambridge University Press.

Thorand, S. (2022). Testing statistical hypotheses using parametric tests. GRIN Verlag.

Vinayachandran, P. N., & Mathew, S. (2003). Phytoplankton bloom in the Bay of Bengal during the northeast monsoon and its intensification by cyclones. *Geophysical Research Letters, 30*(11), 1572. https://doi.org/10.1029/2002GL016717

Vinayachandran, P. N., Murty, V. S. N., & Ramesh Babu, V. (2002). Observations of barrier layer formation in the Bay of Bengal during the summer monsoon. *Journal of Geophysical Research: Oceans, 107*(C12), 8018. https://doi.org/10.1029/2001JC000831

Vissa, N. K., Satyanarayana, A. N. V., & Kumar, B. P. (2013). Response of upper ocean and impact of barrier layer on Sidr cyclone induced sea surface cooling. *Ocean Science Journal, 48*(3), 279–288. https://doi.org/10.1007/s12601-013-0026-x

Walker, N. D., Leben, R. R., & Balasubramanian, S. (2005). Hurricane-forced upwelling and chlorophyll a enhancement within cold-core cyclones in the Gulf of Mexico. *Geophysical Research Letters, 32*(18). https://doi.org/10.1029/2005GL023716

Wang, G., Wu, L., Johnson, N. C., & Ling, Z. (2016). Observed three-dimensional structure of ocean cooling induced by Pacific tropical cyclones. *Geophysical Research Letters, 43*(14), 7632–7638. https://doi.org/10.1002/2016GL069605

Wang, S., Song, J., Guo, J., Fu, Y., Cai, Y., & Wang, L. (2024). The investigation of the response mechanism of SST and chlorophyll to super typhoon "Rey" in the South China Sea. *Water, 16*(4), 603. https://doi.org/10.3390/w16040603

Webster, P. J., Holland, G. J., Curry, J. A., & Chang, H.-R. (2005). Changes in tropical cyclone number, duration, and intensity in a warming environment. *Science, 309*(5742), 1844–1846. https://doi.org/10.1126/science.1116448

World Bank. (2023, August 7). *Extremely severe cyclonic storm mocha, May 2023, Myanmar: Global Rapid Post-Disaster*

Damage Estimation (GRADE) Report. https://www.worldbank.org/en/country/myanmar/publication/global-rapid-post-disaster-damage-estimation-grade-report

World Meteorological Organization. (2025). *Tropical cyclone*. Retrieved from https://wmo.int/topics/tropical-cyclone

Xia, C., Lü, H., Huang, H., Xia, Y., Chen, Z., Ding, X., & Ning, W. (2023). Drastic hydrodynamic changes in the western Bay of Bengal caused by tropical cyclone Nada. *Journal of Sea Research, 194*, 102409. https://doi.org/10.1016/j.seares.2023.102409

Yu, J., Lv, H., Tan, S., & Wang, Y. (2023). Tropical cyclone-induced sea surface temperature responses in the northern Indian Ocean. *Journal of Marine Science and Engineering, 11*(11), 2196. https://doi.org/10.3390/jmse11112196

Zhang, Y., Yue, S., Xu, K., Zhang, Z., Zhou, L., & Zhang, Y. (2023). Performance analysis of global HYCOM flow field using Argo profiles. *International Journal of Digital Earth, 16*(1), 3536–3559. https://doi.org/10.1080/17538947.2023.2252407

Zhao, Z., Zhou, J., & Du, H. (2022). Artificial Intelligence powered forecast of oceanic mesoscale phenomena: A typhoon cold wake case occurring in Northwest Pacific Ocean. *Future Generation Computer Systems, 129*(C), 389–398. https://doi.org/10.1016/j.future.2021.10.031